JACC: CARDIOVASCULAR IMAGING VOL. 15, NO. 7, 2022

ORIGINAL RESEARCH

Clinical Validation of a Virtual Planner for Coronary Interventions Based on Coronary CT Angiography

Jeroen Sonck, MD,[a,b] Sakura Nagumo, MD, PhD,[a,c] Bjarne L. Norgaard, MD, PhD,[d] Hiromasa Otake, MD, PhD,[e] Brian Ko, MD, PhD,[f] Jinlong Zhang, MD,[g] Takuya Mizukami, MD, PhD,[a,h] Michael Maeng, MD, PhD,[d] Daniele Andreini, MD, PhD,[i,j] Yu Takahashi, MD, PhD,[e] Jesper Møller Jensen, MD, PhD,[d] Abdul Ihdayhid, MD, PhD,[f] Ward Heggermont, MD, PhD,[a] Emanuele Barbato, MD, PhD,[a,b] Niya Mileva, MD,[a] Daniel Munhoz, MD,[a,b,k] Jozef Bartunek, MD, PhD,[a] Adam Updegrove, PhD,[l] Amy Collinsworth, MS,[l] Martin Penicka, MD, PhD,[a] Lieven Van Hoe, MD,[m] Jonathon Leipsic, MD, PhD,[n] Bon-Kwon Koo, MD, PhD,[g] Bernard De Bruyne, MD, PhD,[a,o] Carlos Collet, MD, PhD[a]

ABSTRACT

BACKGROUND Low fractional flow reserve (FFR) values after percutaneous coronary intervention (PCI) carry a worse prognosis than high post-PCI FFR values. Therefore, the ability to predict post-PCI FFR might play an important role in procedural planning. Post-PCI FFR values can now be computed from pre-PCI coronary computed tomography angiography (CTA) using the fractional flow reserve derived from coronary computed tomography angiography revascularization planner (FFR_{CT} Planner).

OBJECTIVES The aim of this study was to validate the accuracy of the FFR_{CT} Planner.

METHODS In this multicenter, investigator-initiated, prospective study, patients with chronic coronary syndromes and significant lesions based on invasive FFR ≤0.80 were recruited. The FFR_{CT} Planner was applied to the fractional flow reserve derived from coronary computed tomography angiography (FFR_{CT}) model, simulating PCI. The primary objective was the agreement between the predicted post-PCI FFR by the FFR_{CT} Planner and measured post-PCI FFR. Accuracy of the FFR_{CT} Planner's luminal dimensions was assessed by using post-PCI optical coherence tomography as the reference.

RESULTS Overall, 259 patients were screened, with 120 patients (123 vessels) included in the final analysis. The mean patient age was 64 ± 9 years, and 24% had diabetes. Measured FFR post-PCI was 0.88 ± 0.06, and the FFR_{CT} Planner FFR was 0.86 ± 0.06 (mean difference: 0.02 ± 0.07 FFR unit; limits of agreement: -0.12 to 0.15). Optical coherence tomography minimal stent area was 5.60 ± 2.01 mm^2, and FFR_{CT} Planner minimal stent area was 5.0 ± 2.2 mm^2 (mean difference: 0.66 ± 1.21 mm^2; limits of agreement: -1.7 to 3.0). The accuracy and precision of the FFR_{CT} Planner remained high in cases with focal and diffuse disease and with low and high calcium burden.

CONCLUSIONS The FFR_{CT}-based technology was accurate and precise for predicting FFR after PCI. (Precise Percutaneous Coronary Intervention Plan Study [P3]; NCT03782688) (J Am Coll Cardiol Img 2022;15:1242-1255) © 2022 The Authors. Published by Elsevier on behalf of the American College of Cardiology Foundation. This is an open access article under the CC BY license (http://creativecommons.org/licenses/by/4.0/).

From the [a]Cardiovascular Center Aalst, OLV Clinic, Aalst, Belgium; [b]Department of Advanced Biomedical Sciences University Federico II, Naples, Italy; [c]Department of Cardiology, Showa University Fujigaoka Hospital, Kanagawa, Japan; [d]Department of Cardiology, Aarhus University Hospital, Aarhus, Denmark; [e]Division of Cardiovascular Medicine, Department of Internal Medicine, Kobe University Graduate School of Medicine, Kobe, Japan; [f]Monash Cardiovascular Research Centre, Monash University and Monash Heart, Monash Health, Clayton, Victoria, Australia; [g]Department of Internal Medicine and Cardiovascular

ISSN 1936-878X https://doi.org/10.1016/j.jcmg.2022.02.003

The degree of functional revascularization achieved by percutaneous coronary intervention (PCI) can be quantified by measuring fractional flow reserve (FFR) immediately after stent implantation. Functional revascularization modulates the relationship between PCI and adverse events.[1-3] Patients with high FFR values after PCI have been shown to have a better prognosis than patients with low post-PCI FFR.[4-7] Notably, after an angiographically successful PCI, FFR values remain suboptimal in almost one-third of patients.[6,8] Therefore, tools that aid in achieving functional revascularization have the potential to improve PCI outcomes.

Coronary computed tomography angiography (CTA) is a noninvasive method that allows for anatomical evaluation of the entire coronary tree. In addition, by performing blood flow simulations using computational fluid dynamics, it is possible to derive FFR from coronary CTA images (FFR_{CT}).[9] The FFR_{CT} Planner is a novel tool that allows for virtual stenting of coronary stenoses and prediction of post-PCI FFR.[10] The ability to predict post-PCI FFR might play an important role in patient selection and procedural planning. The present study aimed at validating the accuracy and precision of the FFR_{CT} Planner in predicting post-PCI FFR.

METHODS

STUDY DESIGN. The design of the P3 (Precise Percutaneous Coronary Intervention Plan) study has been reported previously.[10] Briefly, the P3 study was an investigator-initiated, multicenter, prospective study of patients with chronic coronary syndromes referred for PCI. All patients had a coronary CTA performed before the invasive procedure. Patients underwent a comprehensive invasive protocol using a motorized device to record pressure drops along the epicardial vessel, allowing for the standardization of the pressure-length relationship both pre-PCI and post-PCI. In addition, optical coherence tomography (OCT), performed before and after stenting, allowed for matched morphologic evaluation. The study protocol was approved by the investigational review board or ethics committee at each participating center. All patients signed informed consent before the study procedures. The protocol was registered as NCT03782688. Details of the organization of the study are provided in Supplemental Table 1.

The study's primary objective was the agreement between predicted FFR derived from the FFR_{CT} Planner and invasively measured post-PCI FFR. Specifically, 1 FFR_{CT} value extracted from the FFR_{CT} Planner at the same locations as the post-PCI invasive measurements was used for analysis. Secondary objectives included the agreement between FFR values extracted along the coronary vessel from the virtual and invasive post-PCI pullback curves and the agreement between the post-PCI minimal stent area (MSA) from the FFR_{CT} Planner and OCT.

STUDY ELIGIBILITY AND PROCEDURES. Patients with a coronary CTA performed within the standard of care, showing a significant epicardial lesion (defined as diameter stenosis >50% at coronary CTA), were considered for inclusion. Final eligibility was confirmed in the catheterization laboratory after invasive measurement showed FFR ≤0.80. Patients with severely calcified vessels, bifurcation or ostial lesions, left main disease, severe vessel tortuosity, previous revascularization, and atrial fibrillation were excluded. Complete details of the inclusion and exclusion criteria are provided in Supplemental Table 2.

Patients were consented to undergo a PCI protocol requiring pre- and post-stent evaluation using a motorized device for invasive FFR pullbacks and OCT for PCI guidance and stent optimization. Coronary CTA was processed for FFR_{CT} (HeartFlow Inc). Invasive morphologic and functional data were centrally

ABBREVIATIONS AND ACRONYMS

CAD = coronary artery disease

CTA = computed tomography angiography

FFR = fractional flow reserve

FFR_{CT} = fractional flow reserve derived from coronary computed tomography angiography

FFR_{CT} Planner = fractional flow reserve derived from coronary computed tomography angiography revascularization planner

MACE = major adverse cardiac events

MI = myocardial infarction

MSA = minimal stent area

OCT = optical coherence tomography

PCI = percutaneous coronary intervention

PPG = pullback pressure gradient

Center, Seoul National University Hospital, Seoul, South Korea; [h]Division of Clinical Pharmacology, Department of Pharmacology, Showa University School of Medicine, Tokyo, Japan; [i]Centro Cardiologico Monzino, IRCCS, Milan, Italy; [j]Department of Clinical Sciences and Community Health, Cardiovascular Section, University of Milan, Milan, Italy; [k]Department of Internal Medicine, Discipline of Cardiology, University of Campinas (Unicamp), Campinas, Brazil; [l]HeartFlow Inc, Redwood City, California, USA; [m]Department of Radiology, OLV Clinic, Aalst, Belgium; [n]Department of Medicine and Radiology, University of British Columbia, Vancouver, British Columbia, Canada; and the [o]Department of Cardiology, University Hospital of Lausanne, Lausanne, Switzerland.

Harvey Hecht, MD, served as Guest Editor for this paper.

The authors attest they are in compliance with human studies committees and animal welfare regulations of the authors' institutions and Food and Drug Administration guidelines, including patient consent where appropriate. For more information, visit the Author Center.

Manuscript received September 27, 2021; revised manuscript received January 31, 2022, accepted February 3, 2022.

FIGURE 1 Study Flowchart

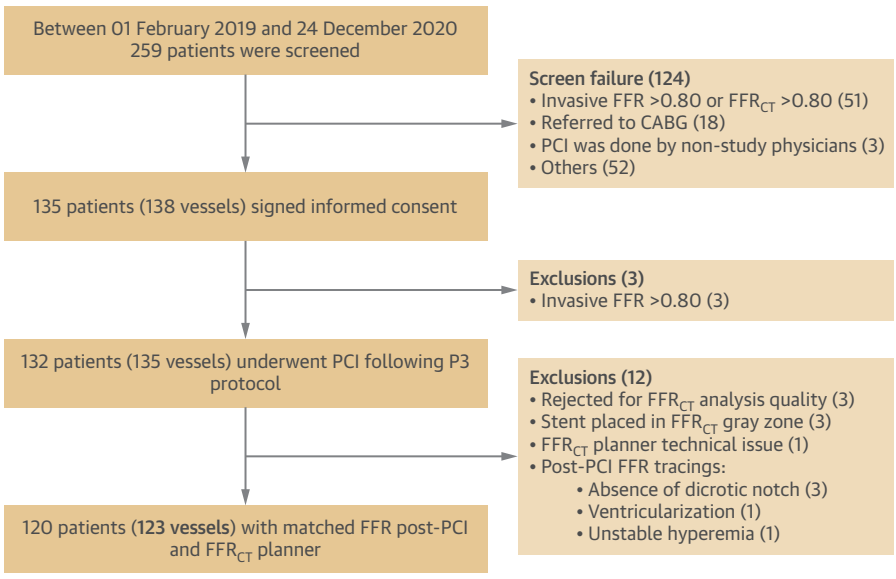

Gray zone refers to the segment of the fractional flow reserve derived from coronary computed tomography angiography (FFR$_{CT}$) images model with <1.8 mm in diameter where the FFR$_{CT}$ values are not displayed. CABG = coronary artery bypass grafting; FFR = fractional flow reserve; FFR$_{CT}$ Planner = fractional flow reserve derived from coronary computed tomography angiography revascularization planner; PCI = percutaneous coronary interventions.

analyzed by a core laboratory (CoreAalst BV) blinded to the FFR$_{CT}$ Planner results.

CORONARY CTA IMAGE ACQUISITION AND ANALYSIS. Coronary CTA was performed by using the latest generation CT scanners. Local imaging acquisition guidelines were followed with the recommendation to use nitrates before CT imaging acquisition and beta-blockers in cases of heart rate >65 beats/min. Image quality was adjudicated by using the 4-point Likert scale at the per-vessel level by an independent CT image quality committee. The effective radiation dose was calculated by using conversion coefficient 0.014. Definitions of CT image quality are shown in Supplemental Table 3. Calcium scores were calculated according to the Agatston method at per-patient and per-vessel levels. Calcium burden was defined as the ratio between calcium volume and plaque volume in the lesion.[11] Luminal dimensions were extracted from the FFR$_{CT}$ and FFR$_{CT}$ Planner models. Plaque volume and composition were analyzed by using validated software (QAngio CT, Medis Medical Imaging).

FFR$_{CT}$ PLANNER. The FFR$_{CT}$ Planner is a novel tool that predicts FFR in response to changes to patient-specific lumen geometry in real time. The FFR$_{CT}$ Planner works on a touchscreen display allowing the user to manually select the segment of the vessel to be dilated. The FFR$_{CT}$ Planner automatically identifies the position of the lesion(s) with area stenosis >30% by placing a marker (white circle). The length is not fixed and depends on the stenosis. The proximal and distal ends of the automatic length are set where the lumen recovers to 10% stenosis. The user can adapt the length by extending and reducing the proposed length, resulting in several treatment strategies with different stent lengths. The length selected is provided by the tool. Dilation of the FFR$_{CT}$ model (or virtual stenting) is performed by automatically changing the local radius to the ideal target radius based on proximal and distal reference segments. Diameter information is not provided in the current version of the FFR$_{CT}$ Planner. Lumen geometric changes influence the flow rate through the model to calculate the new FFR$_{CT}$ along the vessel. The FFR$_{CT}$ Planner is a single-vendor commercial product (HeartFlow Inc). Of note, application of the FFR$_{CT}$ Planner to ostial lesions or vessels <1.8 mm in diameter is not supported by the current version.

In the present study, the FFR$_{CT}$ Planner was applied by using the stent position recorded during the invasive procedure. The FFR$_{CT}$ Planner was used blinded to the invasive data. In addition, virtual FFR$_{CT}$ pullback curves were created, extracting 1

FFR_{CT} value every 0.1 mm from the pre- and post-PCI FFR_{CT} models.[12] FFR_{CT} Planner-derived luminal information was used to calculate the MSA. FFR_{CT} Planner-derived stent expansion was defined as the ratio between MSA and average reference lumen areas.

For the primary endpoint, 1 FFR_{CT} value extracted from the FFR_{CT} Planner at the post-PCI invasive measurement location was used for analysis. For the secondary endpoint, the MSA in the virtually stented segment in the FFR_{CT} Planner was used for comparison with the MSA derived from OCT.

INVASIVE PROCEDURE. After administering intracoronary nitroglycerin, coronary angiograms were acquired in 2 projections separated by at least 30°. Three-dimensional quantitative coronary angiography was performed by using CAAS 8.2 Software (Pie Medical Imaging). Two angiographic projections separated by at least 30° were acquired. These projections were then used to create a 3-dimensional reconstruction of the coronary artery pre- and post-PCI. Adjudication of lesion complexity was performed by using American Heart Association/American College of Cardiology classification by the independent core laboratory.

FFR measurements were performed following the recommendations of the Standardization of Fractional Flow Reserve Measurements document.[13] The pressure wire sensor was positioned in distal coronary segments >2 mm in diameter by visual estimation. Pressure wire position was recorded by using contrast injection to identify the pullback start position. A continuous intravenous adenosine infusion was given at a dose of 140 mg/kg per minute via a peripheral or central vein to obtain steady-state hyperemia for at least 2 minutes. A pullback device (Volcano R 100, Volcano Corporation), adapted to grip the coronary pressure wire (PressureWire X, Abbott Vascular), was set at a speed of 1 mm/s to pull back the pressure wire sensor up to the tip of the guiding catheter during continuous pressure recording. The maximal pullback length was 130 mm per vessel. If FFR drift (>0.03) was observed, the FFR pullback was repeated. FFR was defined as the lowest ratio between distal and proximal coronary pressures during hyperemia. The functional gain was defined as the difference between post- and pre-PCI FFR. The pullback pressure gradient (PPG) was calculated from the FFR pullback curves. The PPG is a novel metric that discriminates between focal and diffuse coronary artery disease (CAD). PPG values close to 1 represent focal CAD, whereas values close to 0 indicate diffuse disease.[14] The PPG was not calculated from FFR_{CT} because the formula uses a threshold to detect diffuse disease below the FFR_{CT} unit's resolution. The position of the invasive FFR sensor was recorded and matched with the location of the FFR_{CT} measurement.

FFR gradients were further compared in 3 segments (proximal, stent, and distal). The proximal gradient was defined as the FFR gradient measured between the ostium of the vessel and the proximal stent edge (FFR ostium minus FFR proximal stent edge). Stent gradients were defined as FFR gradient from the proximal to the distal stent edges. The distal gradient was defined as the FFR gradient observed from the distal stent edge to the pressure wire sensor position (FFR distal stent edge minus FFR at the distal pressure sensor position). Details of the co-pressure

TABLE 1 Baseline Clinical and Coronary CTA Characteristics (N = 120)

Age, y	64.33 ± 8.97
Male	95 (79.2)
BMI, kg/m^2	26.87 ± 3.30
Dyslipidemia	95 (79.2)
Hypertension	70 (58.3)
Diabetes mellitus	29 (24.2)
Current smoker	28 (23.3)
Previous PCI in nontarget vessel	5 (4.2)
Peripheral artery disease	6 (5.0)
Clinical presentation	
Silent ischemia	28 (23.3)
Stable angina CCS I	37 (30.8)
Stable angina CCS II	44 (36.7)
Stable angina CCS III	8 (6.7)
Stable angina CCS IV	1 (0.8)
Unstable angina	2 (1.7)
Creatinine, mg/dL	0.94 ± 0.20
LVEF	60.01 ± 6.43
No. of vessels	123
LAD	94 (76.4)
LCX	13 (10.6)
RCA	16 (13.0)
Lesion length, CT image, mm	47.76 ± 20.97
Minimum lumen area, CT image, mm^2	1.82 ± 0.98
Diameter stenosis, CT image, %	51 ± 14
Area stenosis, CT image, %	74 ± 15
Plaque burden, CT image, %	85 ± 9
Calcium burden, CT image, %	0.19 ± 0.17
Calcium score per patient	516.53 ± 705.37
Calcium score, treated vessel	228.2 ± 340.7
Invasive pre-PCI FFR	0.64 ± 0.13
FFR_{CT}	0.64 ± 0.11

Values are mean ± SD or n (%), unless otherwise indicated.

BMI = body mass index; CCS = Canadian Cardiovascular Society; CT = computed tomography; CTA = computed tomography angiography; FFR = fractional flow reserve; FFR_{CT} = fractional flow reserve derived from coronary computed tomography angiography; LAD = left anterior descending; LCX = left circumflex; LVEF = left ventricular ejection fraction; PCI = percutaneous coronary intervention; RCA = right coronary artery.

gradient co-registration procedure have been described elsewhere.[10] Pressure tracings were examined by the core laboratory to evaluate quality, curve artifacts, and hyperemia stability. Pressure tracings and pullback curves were analyzed by using CoroFlow version 3.5 (Coroventis Research).

Subsequently, OCT pullbacks of 75 mm were acquired by using the Dragonfly OPTIS Imaging Catheter (Abbott Vascular). OCT was mandated before and after stent implantation. OCT analyses were performed at the lesion level. An automated algorithm defined minimal lumen area. Cases in which OCT was performed after pre-dilatation were excluded from the minimal lumen area analysis. Plaque analysis was performed as previously described.[15] Stent expansion was defined as the ratio between MSA and average reference lumen area. OCT images were analyzed by the core laboratory using CAAS IntraVascular version 2.1 (Pie Medical Imaging).

PCI procedures were guided by FFR and OCT pullbacks. The FFR_{CT} Planner did not influence the invasive procedure. Stent optimization, based either on FFR or OCT, was left to the operator's discretion. Cardiac enzymes and an electrocardiogram were collected 6 to 24 hours after the procedure. Clinical follow-up was performed at 1 year after the procedure. Major adverse cardiac events (MACE) were defined as cardiac death, target vessel myocardial infarction (MI), or target vessel ischemia-driven revascularization. Peri-procedural MI was defined according to the Fourth Universal Definition of Myocardial Infarction.[9] A clinical events committee independently adjudicated all adverse events.

STATISTICAL ANALYSIS. Continuous variables with normal distribution are presented as mean ± SD and non-normally distributed variables as median (IQR). Categorical variables are presented as counts and percentages. The primary objective was the agreement between the FFR_{CT} Planner and co-localized invasively measured post-PCI FFR assessed by using the Bland-Altman method.[16] The mean difference was considered a metric of accuracy, and the SD of the mean difference a metric of precision. Given the assumption that the difference between the FFR_{CT} Planner and invasive post-PCI FFR would be ≤0.04 FFR unit, with an SD of 0.07, we estimated that 127 patients would provide 80% power (at a 2-sided 0.05 alpha level) to detect a mean difference of 0.04 with an SD of <0.07 between the predicted FFR_{CT} Planner and invasively measured post-PCI FFR based on the Bland-Altman method, foreseeing an attrition rate of 2.5%.[17] Disease complexity was stratified based on the pattern of CAD (ie, focal vs diffuse) and on the calcium burden (ie, high vs low). The median values of the PPG and calcium burden were used to divide the groups. Student's *t*-tests were used to compare the performance of the FFR_{CT} Planner stratified according to CAD complexity. Performance of the FFR_{CT} Planner, in with different levels of image quality according to the Likert score was compared by using analysis of variance. Logistic regression analysis was used to assess the relationship between pre- and post-FFR values and adverse events. In addition, rates of MACE were compared between high and low FFR values stratified by the median. All analyses were performed by using R statistical software (version 4.0.5, R Foundation for Statistical Computing).

TABLE 2 Invasive Procedural Characteristics

Radial access	110 (89.4)
No. of vessels	123
No. of angiographic lesions	129
Lesion type	
Type A	37 (28.7)
Type B1	30 (23.3)
Type B2	29 (22.5)
Type C	33 (25.6)
Lesion length, QCA, mm	24.4 ± 14.1
Mean reference lumen area, QCA, mm^2	5.91 ± 2.26
Minimal lumen area, QCA, mm^2	1.48 ± 0.98
Diameter stenosis, QCA, %	51.0 ± 14.5
Area stenosis, QCA, %	73.9 ± 15.06
OCT pre-PCI	116 (90)
Lesion length OCT, mm[a]	31.2 ± 14.1
Mean reference luminal area, OCT, mm^2[,a]	7.27 ± 2.73
Minimal luminal area, OCT, mm^2[,a]	1.79 ± 0.75
Area stenosis, OCT, %[a]	48.92 ± 11.7
Pre-dilatation	114/129 (89.1)
Post-dilatation	111/129 (86.7)
Stents per vessel, n	1.33 ± 0.57
Stents per lesion, n	1.26 ± 0.53
OCT post-PCI	115/129 (97.5)
Total stent length, mm	36.8 ± 17.1

Values are n (%) or mean ± SD, or n/N (%), unless otherwise indicated. [a]Quantitative analysis performed only in cases with optical coherence tomography (OCT) imaging before pre-dilatation (n = 74).

PCI = percutaneous coronary intervention; QCA = quantitative coronary angiography.

RESULTS

From February 2019 to December 2020, a total of 259 patients with a severe epicardial lesion on coronary CTA were screened for eligibility at 5 centers in 5 countries. **Figure 1** shows the flowchart of the study (details of screen failures are shown in Supplemental Table 4). A total of 120 patients (123 vessels) were included in the final analysis.

BASELINE CHARACTERISTICS. Table 1 shows the baseline clinical and coronary CTA characteristics. The mean radiation dose (effective dose) was 5.64 ± 4.1 mSv. Coronary CTA image quality was assessed as good or excellent in 93% of the patients. The types of CT scanners used in the study are shown in Supplemental Table 5. Invasive angiography identified 129 stenoses; 48.1% were complex lesions (ie, B2/C according to American College of Cardiology/American Heart Association lesion classification). Table 2 shows the quantitative coronary angiography characteristics. The minimal lumen area according to OCT was 1.79 ± 0.75 mm^2.

Mean resting distal coronary pressure/aortic coronary pressure was 0.83 ± 0.13, whereas mean FFR was 0.66 ± 0.13. Details on invasive physiology tracing analysis adjudication are presented in Supplemental Figures 1 and 2. Agreement between pre-PCI invasive FFR and FFR_{CT} is shown in Supplemental Figure 3. FFR pullbacks pre-PCI were available in 97 vessels. The mean FFR pullback length was 102.8 ± 19.8 mm. The mean PPG was 0.66 ± 0.13, and the mean translesional FFR gradient was 0.27 ± 0.15 units. Procedural characteristics are shown in Table 2.

PRIMARY ENDPOINT. After PCI, the mean FFR_{CT} derived from the FFR_{CT} Planner was 0.86 ± 0.06, whereas the mean invasive post-PCI FFR was 0.88 ± 0.06, with a mean difference of 0.02 and an SD of 0.07 (limits of agreement: -0.12 to 0.15) (Figure 2). The functional gain derived from the FFR_{CT} Planner and invasive FFR was 0.22 ± 0.12 and 0.22 ± 0.14, respectively (mean difference: 0.00; SD: 0.13; limits of agreement: -0.26 to 0.26) (Supplemental Figure 4). The accuracy of the FFR_{CT} Planner to predict post-PCI FFR ≤0.80 and ≤0.90 was 83% and 71%, respectively. The accuracy of the FFR_{CT} Planner stratified according to pre-PCI FFR, post-PCI FFR, and by vessel type is shown in Supplemental Tables 6 and 7 and Supplemental Figure 5. After PCI, 97,402 FFR values along 98 coronary vessels were matched by using the FFR_{CT} and invasive FFR pullback curves. The mean difference at matched locations was 0.01 FFR unit, and the SD was 0.05 (limits of agreement: -0.08 to 0.10) (Figure 3). Post-procedural characteristics are shown in Table 3. The mean difference in stent FFR gradients between invasive FFR and the FFR_{CT} Planner was 0.02, and the SD was 0.03 (limits of agreement: -0.05 to 0.08) (Supplemental Figure 6).

SECONDARY ENDPOINTS. After PCI, quantitative OCT analysis was feasible in 82% (104 of 127) of the lesions. Stent expansion >80% and 90% was observed in 49% and 25% of patients, respectively. Edge dissections were observed in 11.6%; the accuracy of the FFR_{CT} Planner stratified by the presence of edge dissections is shown in Supplemental Table 8. Details of the OCT analysis are presented in Supplemental Figures 7 and 8 and Supplemental Table 9. MSA by OCT was 5.6 ± 2.0 mm^2, whereas MSA predicted by the FFR_{CT} Planner was 5.0 ± 2.2 mm^2 (mean difference: 0.66 mm^2; SD: 1.21; limits of agreement: −1.7 to 3.0) (Figure 4). The agreement on MSA between the FFR_{CT} Planner and OCT stratified according to the pattern of CAD (ie, focal or diffuse) and calcium burden is shown in Supplemental Figures 9 and 10. The agreement between nominal stent size and vessel dimensions at the distal reference diameter derived from the FFR_{CT} model is shown in Supplemental Figure 11. The agreement between FFR_{CT} lesion length and stent length is shown in Supplemental Figure 12. The **Central Illustration** summarizes the study protocol, primary and secondary endpoints.

FIGURE 2 Mean Difference Between FFR_{CT} Planner and Invasive Post-PCI FFR

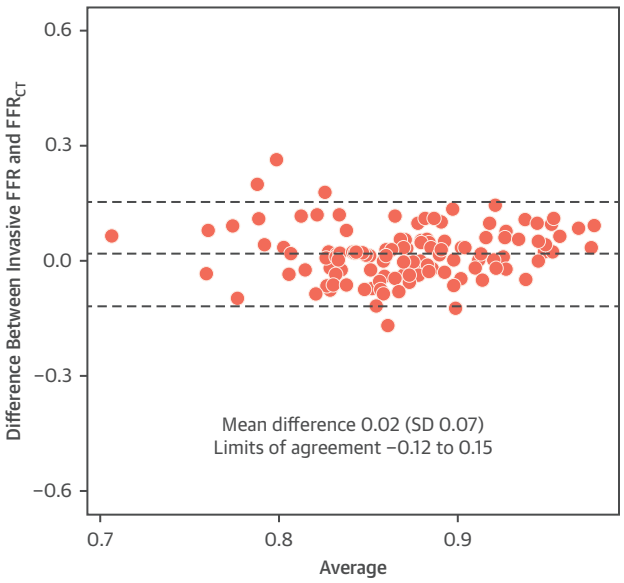

Bland-Altman analysis of the agreement between the FFR_{CT} Planner and invasively measured FFR. Abbreviations as in Figure 1.

ACCURACY OF THE FFR_{CT} PLANNER STRATIFIED ACCORDING TO CAD COMPLEXITY. Patients with predominant focal or diffuse disease were divided by the median PPG value 0.66. As expected, patients with low PPG (diffuse CAD) at baseline had lower post-PCI FFR compared with patients with high PPG (0.86 ± 0.05 vs 0.91 ± 0.07; $P < 0.001$). The FFR_{CT} Planner also predicted significantly lower FFR in patients with low PPG (0.85 ± 0.06 vs 0.87 ± 0.05; $P = 0.048$). The functional gain was significantly greater in patients

FIGURE 3 Mean Difference Between FFR_{CT} Planner and Invasive Post-PCI FFR Pullback Curves

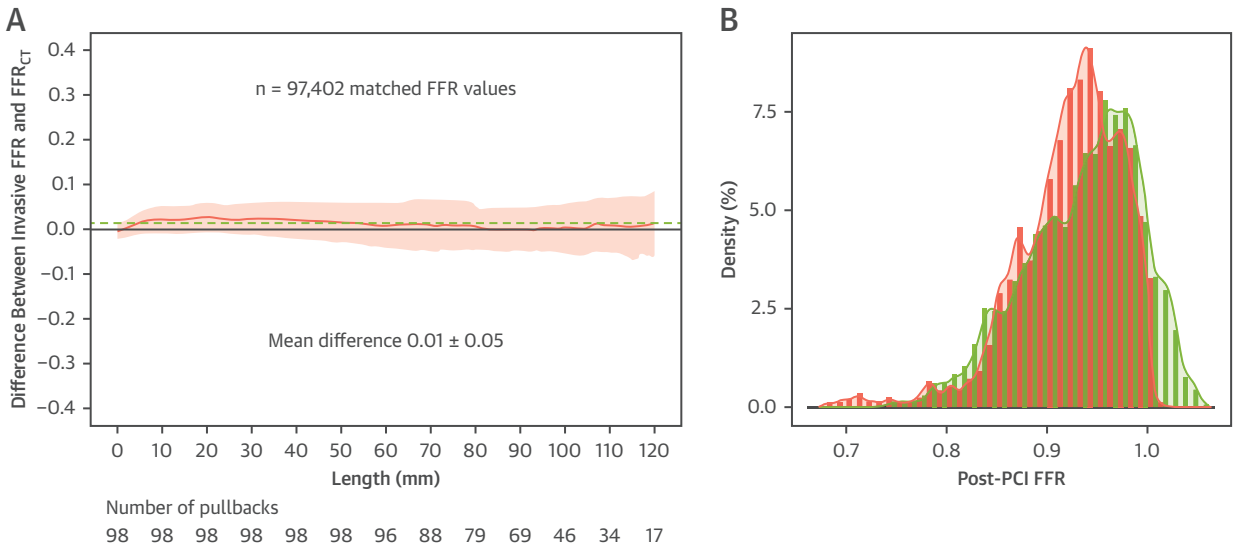

(A) In the x-axis the length of the vessels is shown and the number of pullbacks reaching the given length. The y-axis represents the difference between invasive FFR and FFR_{CT} post-PCI. The **green dashed bar** represents the mean difference in the whole pullback. The **red line** indicates the position-dependent mean difference between invasive FFR and FFR_{CT}. The **shaded red area** depicts the SD of the difference. **(B)** The distribution of post-PCI FFR invasive **(red)** and FFR_{CT} **(red)**. Abbreviations as in Figure 1.

TABLE 3 Post-Procedural Angiographic, Intravascular Imaging, and Functional Characteristics

3D QCA	
Acute gain, mm	1.43 ± 0.56
Residual diameter stenosis, %	2.57 ± 11.19
Minimal stent area, mm^2	6.18 ± 2.11
OCT	
Minimal stent area, $mm^{2,a}$	5.60 ± 2.03
Stent expansion, %[a]	80 ± 18
Invasive pressure measurements	
P_d/P_a at rest[b]	0.95 ± 0.04
Duration of hyperemia, s	222.7 ± 48.8
FFR post-PCI	0.88 ± 0.06
Functional gain	0.22 ± 0.14
Proximal segment pressure gradient, FFR units[c]	0.01 ± 0.03
Stent pressure gradient, FFR units[c]	0.05 ± 0.03
Distal segment pressure gradient, FFR[c]	0.05 ± 0.04
FFR_{CT}	
FFR_{CT} distal	0.86 ± 0.06
Functional gain FFR_{CT}	0.22 ± 0.12
Proximal segment pressure gradient, FFR_{CT} units[c]	0.05 ± 0.03
Stent pressure gradient, FFR_{CT} units[c]	0.03 ± 0.03
Distal segment pressure gradient, FFR_{CT}[c]	0.05 ± 0.05

Values are mean ± SD. [a]Available for 103 lesions. [b]Available for 118 vessels. [c]Available for 109 vessels.

3D = 3-dimensional; P_a = aortic coronary pressure; P_d = distal coronary pressure; other abbreviations as in Tables 1 and 2.

with high PPG (focal CAD) compared with patients with low PPG ($P < 0.001$ for both FFR_{CT} and invasive FFR) (Supplemental Table 10). Case examples of focal and diffuse CAD are shown in Figure 5. The FFR_{CT} Planner's accuracy was similar in cases of diffuse or focal CAD (mean difference between FFR_{CT} Planner and invasive post-PCI FFR in diffuse CAD: 0.01 ± 0.05 vs 0.03 ± 0.08 in focal CAD; $P = 0.057$) (Figure 6).

Patients with high calcium burden had significantly lower invasive post-PCI FFR (0.87 ± 0.06 high calcium burden vs 0.89 ± 0.06 low calcium burden; $P = 0.041$). Post-PCI FFR_{CT} Planner FFR was similar between high and low calcium burden (0.86 ± 0.06 vs 0.87 ± 0.06; $P = 0.537$). The accuracy of the FFR_{CT} Planner was comparable in cases with high and low calcium burden (mean difference between FFR_{CT} Planner and invasive post-PCI FFR in high calcium burden: 0.01 ± 0.07 vs low calcium burden 0.01 ± 0.07; $P = 0.192$) (Supplemental Table 11).

The FFR_{CT} Planner's accuracy was similar across the range of image quality (mean difference between FFR_{CT} Planner and invasive post-PCI FFR in Likert score 2: 0.03 ± 0.08; Likert score 3: 0.02 ± 0.07; Likert score 4: 0.02 ± 0.07; $P = 0.898$) (Supplemental Figure 13).

FIGURE 4 **Correlation and Mean Difference Between MSA Predicted by the FFR_{CT} Planner and Post-PCI MSA Measured by Using OCT**

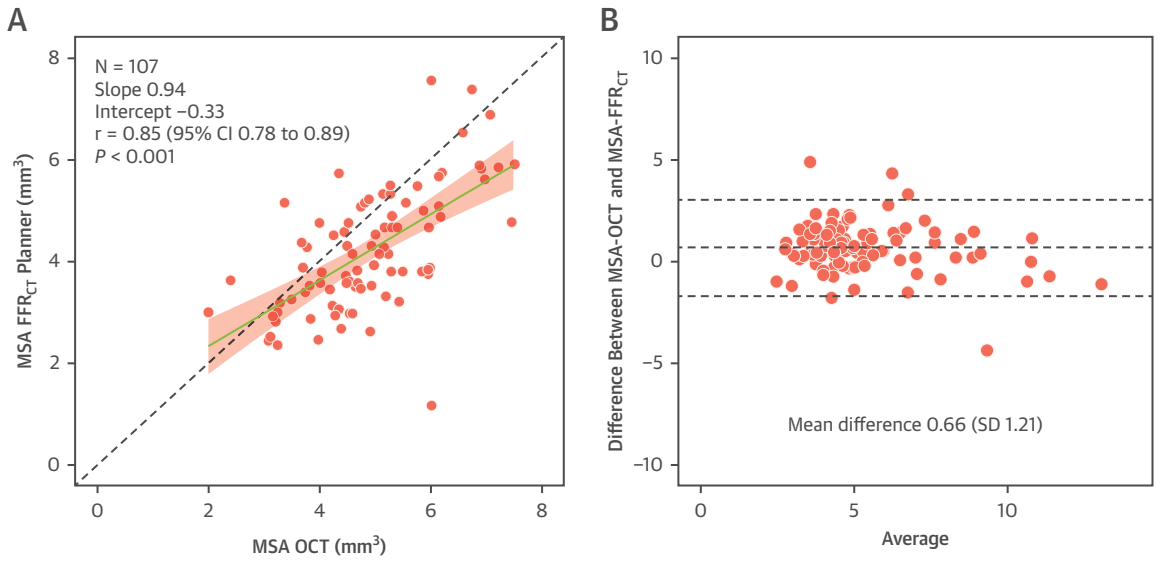

(A) The correlation between minimal stent area (MSA) derived from intravascular optical coherence tomography (OCT) and MSA derived from the FFR_{CT} Planner. **(B)** The Bland-Altman analysis of the agreement on MSA between OCT and FFR_{CT} Planner. Abbreviations as in Figure 1.

CLINICAL OUTCOMES. Median clinical follow-up was 601 days (IQR: 406-583 days). The MACE rate was 15.4%, mainly driven by the periprocedural MI. One patient had a spontaneous MI, and 1 patient had a target vessel revascularization. Neither invasive post-PCI FFR nor FFR_{CT} Planner predicted the occurrence of MACE (OR: 1.02 [95% CI: 0.46-2.29; $P = 0.955$] and 0.67 [95% CI: 0.247-1.60; $P = 0.401$], respectively). Supplemental Table 12 presents rates of MACE stratified according to FFR_{CT} Planner results. FFR_{CT} at baseline and calcium score were associated with MACE. MACE stratified according to baseline FFR_{CT} are presented in Supplemental Table 13. Calcium score per vessel was the only independent predictor of adverse events (predominantly periprocedural MI). Univariate and multivariate analyses are shown in Supplemental Table 14.

DISCUSSION

The present study evaluated the performance of the FFR_{CT} Planner. The main results showed that the FFR_{CT} Planner accurately predicted post-PCI FFR in patients with chronic coronary syndromes. The predicted and observed improvements in epicardial conductance were similar between the FFR_{CT} Planner and invasive FFR. Furthermore, luminal dimensions achieved after stenosis remodeling on the FFR_{CT} model had a substantial agreement with the ones obtained invasively using OCT post-PCI.

The goal of PCI is to re-establish normal epicardial conductance aiming at improving angina, quality of life, and patient outcomes.[18] Post-PCI FFR is an indicator of the degree of functional revascularization.[19] Moreover, FFR measured after PCI has been identified as an independent predictor of target vessel failure.[5] FFR post-PCI is affected by pressure losses in the stented segment and residual atherosclerotic burden proximal and distal to the treated region.[20] In patients with focal CAD, pressure losses are circumscribed within the anatomical stenosis. In these cases, PCI restores conductance, resulting in high post-PCI FFR (Supplemental Case Example 012). Conversely, in patients with diffuse atherosclerosis, pressure losses are distributed along the coronary vessel. PCI in diffuse disease resulted in negligible improvement in vessel conductance (Supplemental Case Example 001); this has been linked with an increased rate of adverse clinical events.[4] Therefore, post-PCI FFR is partly determined by the baseline disease pattern. FFR_{CT} facilitates the identification of diffuse disease. The FFR_{CT} Planner technology leverages this feature, offering the possibility to investigate, using a patient-specific model, the best revascularization strategy in terms of post-PCI FFR before the

CENTRAL ILLUSTRATION **Prospective Validation of the FFR_{CT} Planner**

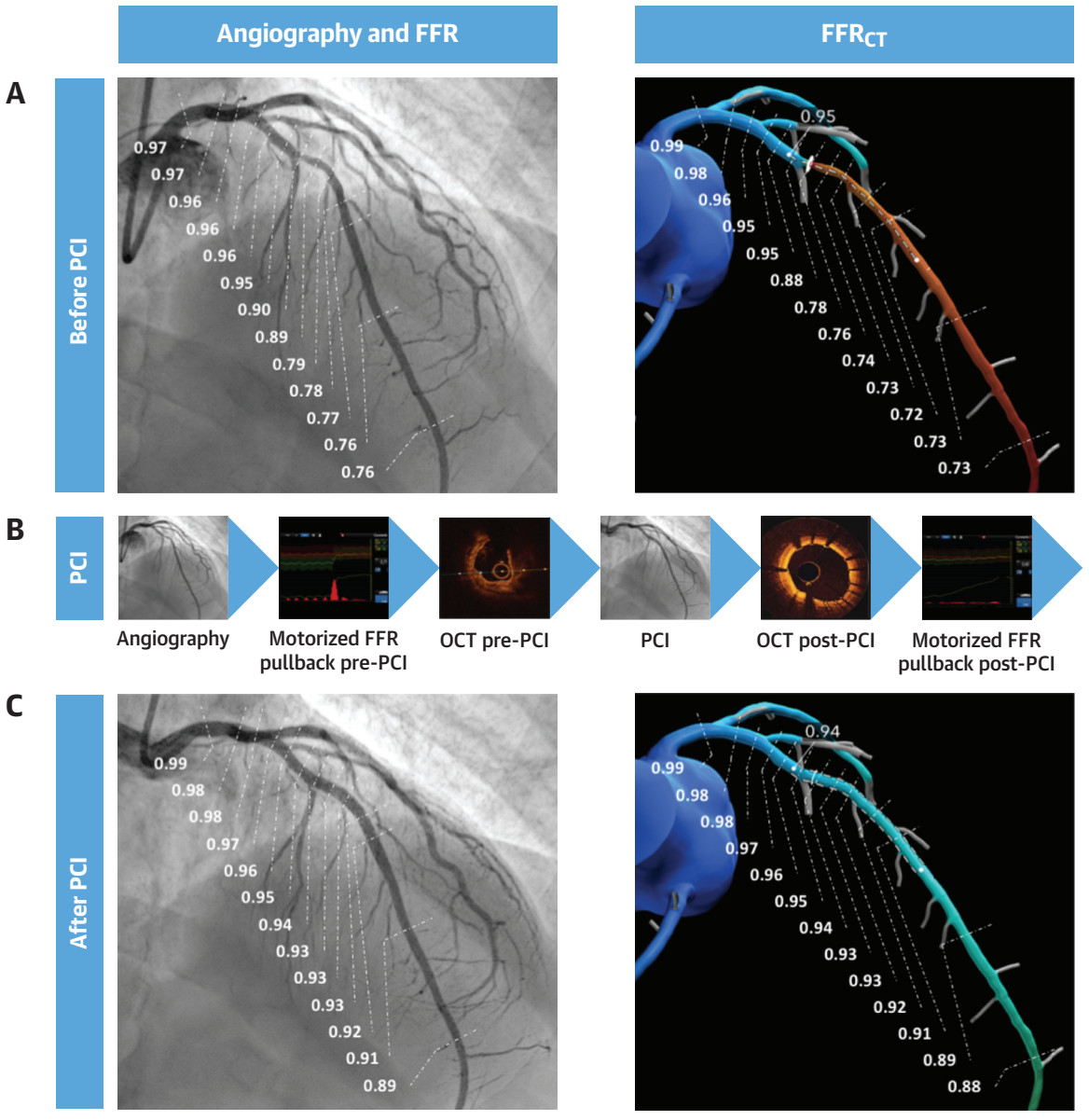

Sonck J, et al. J Am Coll Cardiol Img. 2022;15(7):1242–1255.

(A) The physiological information extracted from the invasive fractional flow reserve (FFR) **(left)** and the fractional flow reserve derived from coronary computed tomography angiography images (FFR_{CT}) **(right)** with matched FFR values along the coronary vessel before percutaneous coronary intervention (PCI). **(B)** The invasive PCI protocol used motorized FFR pullback with pullback pressure gradient (PPG) calculation, followed by optical coherence tomography (OCT) to plan stent implantation. **(C)** After PCI, OCT was repeated for stent optimization, and, finally, FFR followed by a new motorized FFR pullback was performed. Similarly, post-PCI physiological information was extracted along the epicardial vessel, and post-PCI FFR values were matched and compared. The primary objective is shown in the **bottom part of D**, presenting the mean difference between the FFR_{CT} Planner and invasive post-PCI FFR (0.02 ± 0.07 FFR unit). **(E)** The mean difference between the FFR_{CT} Planner and invasive FFR pullbacks at each location in the coronary vessel; the x-axis represents the distance of the FFR value from the coronary ostium. **(F)** The correlation between minimal stent area (MSA) derived from OCT (x-axis) and predicted by using the FFR_{CT} Planner.

Continued on the next page

CENTRAL ILLUSTRATION Continued

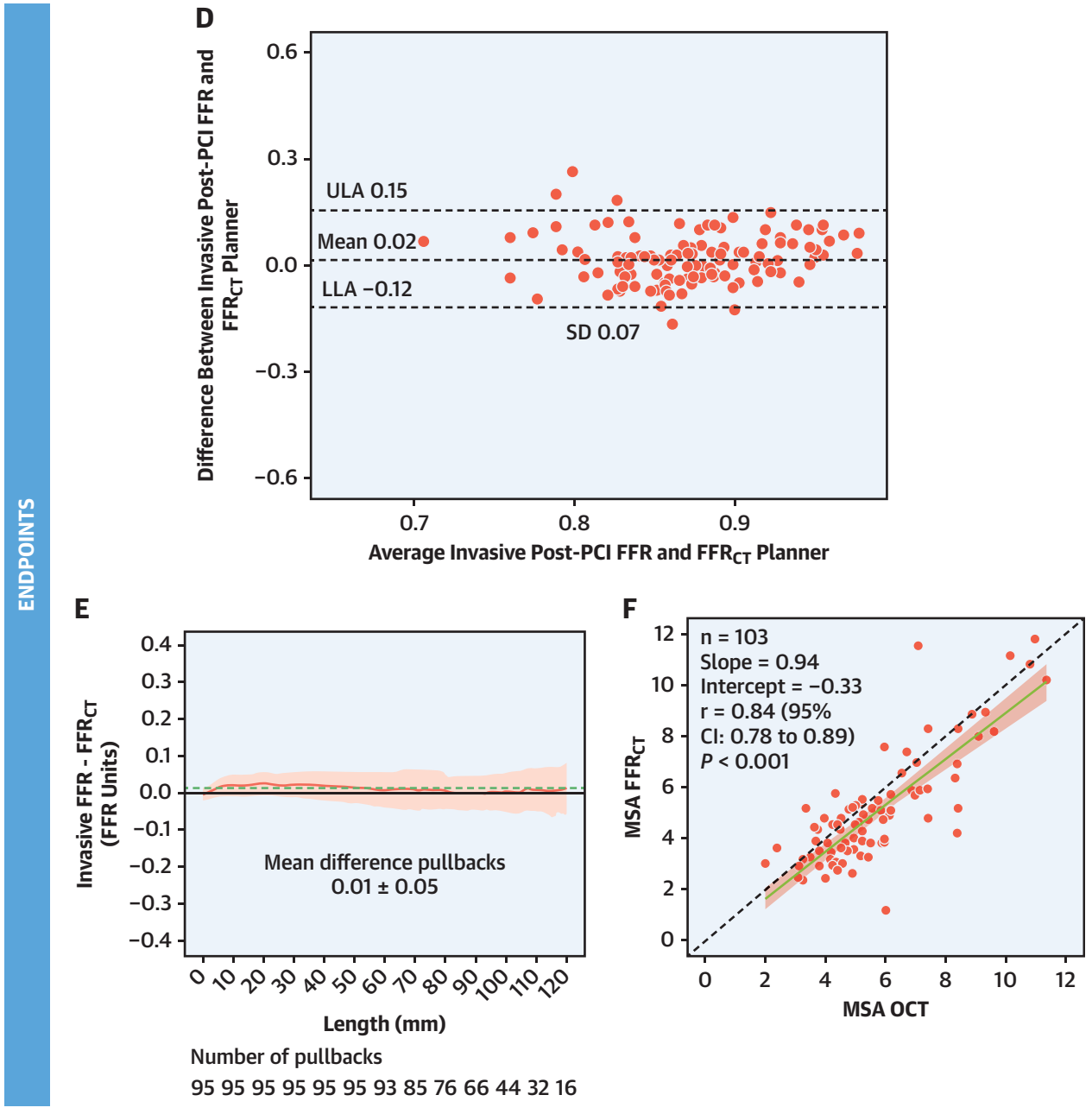

Sonck J, et al. J Am Coll Cardiol Img. 2022;15(7):1242–1255.

invasive procedure. By predicting the improvement in FFR, the FFR_{CT} Planner might be able to identify patients who benefit the most from PCI in terms of angina relief. This hypothesis warrants further investigation.

The ability to predict post-PCI FFR lays a foundation for a novel and personalized approach in patients considered for revascularization. In the present study, we focused on the accuracy and precision of the FFR_{CT} Planner. The mean difference between the FFR_{CT}

FIGURE 5 Case Examples

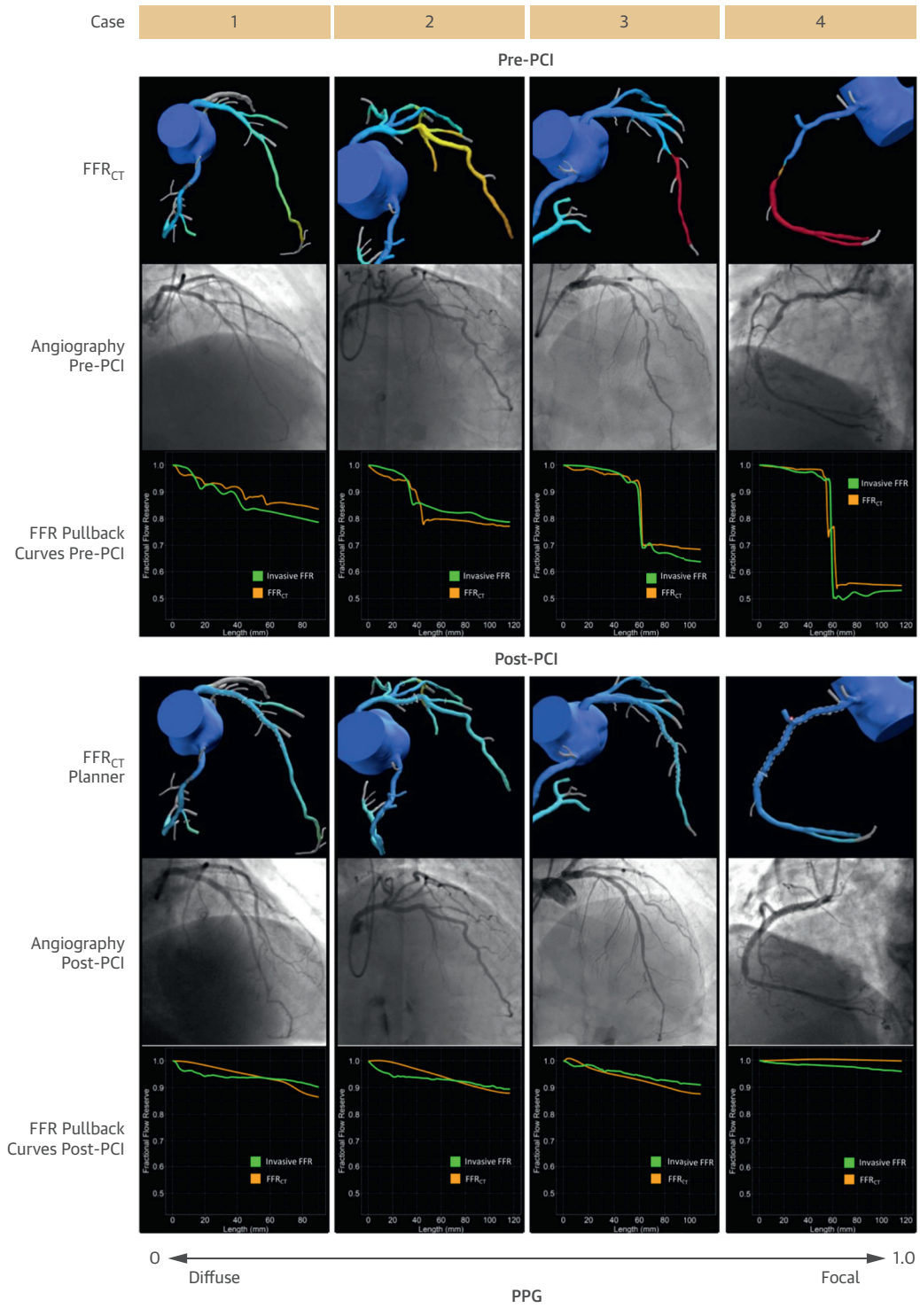

Four case examples with **(from top to bottom)** FFR$_{CT}$, baseline invasive angiography, pre-PCI FFR pullback curves (**orange** FFR$_{CT}$ pullback curve and **green** invasive motorized pullback curve), FFR$_{CT}$ Planner model, post-PCI angiogram, and post-PCI invasive FFR and FFR$_{CT}$ pullback curves. Ranked, from left to right, diffuse to focal coronary artery disease. PPG = pullback pressure gradient; other abbreviations as in Figure 1.

FIGURE 6 Accuracy of the FFR_{CT} Planner Stratified According to Focal or Diffuse CAD and Calcium Burden

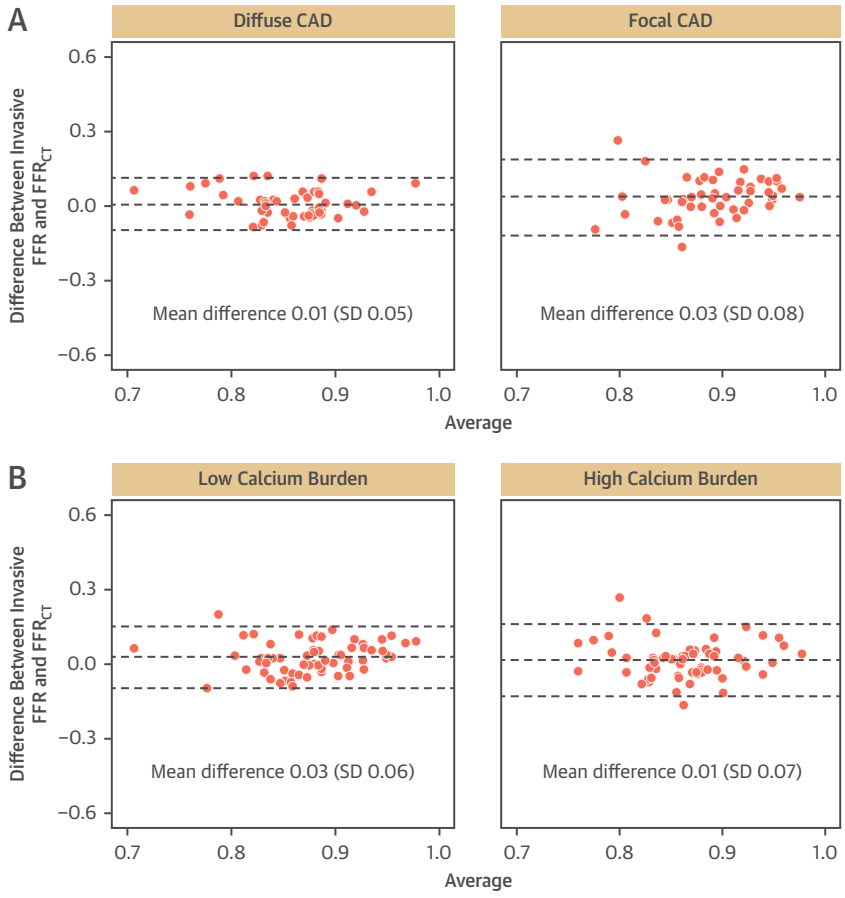

(A) Bland-Altman plots with the mean difference between the FFR_{CT} Planner and post-PCI FFR stratified according to focal or diffuse coronary artery disease (CAD) using the pullback pressure gradient (PPG) index. **(B)** Bland-Altman plots with the mean difference between the FFR_{CT} Planner and post-PCI FFR stratified according to lesion calcium burden. Abbreviations as in Figure 1.

Planner and invasive FFR was 0.02 ± 0.07 unit. The high accuracy and precision of the FFR_{CT} Planner remained independent of the baseline CAD pattern (ie, focal or diffuse), the degree of calcification, and the CT image quality. Interestingly, we observed slightly higher accuracy of the FFR_{CT} Planner in cases of diffuse CAD. This finding is partly explained by the greater magnitude of FFR change in cases with focal CAD leading to a larger numerical difference in the absolute post-PCI FFR value. By protocol, stents were optimized by OCT, ensuring the best possible expansion. PCI guided by OCT results in higher post-PCI FFR, mainly by reducing trans-stent pressure gradients.[21] This study combined FFR and OCT pullbacks for stent optimization, providing a state-of-the-art approach to PCI.[22] This is one of the main differences with previous retrospective studies that have reported lower accuracy of the FFR_{CT} Planner.[17,23] This level of scrutiny was required to evaluate the performance of the FFR_{CT} Planner under optimal PCI conditions.

In the present study, despite intravascular imaging-guided stent optimization, 12% of the patients remained with a post-PCI FFR ≤0.80. Nonetheless, the rate of adverse events outside the periprocedural window was very low (1.5% [2 of 120]). Neither invasive nor FFR_{CT} Planner-derived post-PCI FFR was associated with adverse clinical outcomes. Conversely, low FFR_{CT} pre-PCI, reflecting higher severity of CAD, and calcium score were associated with MACE, mainly related to the occurrence of periprocedural MI. It is important to highlight that the present study was not powered to evaluate clinical

outcomes; instead, we aimed at validating the accuracy of the tool to predict post-PCI FFR. The mean difference (bias) between the FFR_{CT} Planner and invasively measured post-PCI FFR was 0.02 FFR unit with limits of agreement ranging from -0.12 to 0.15; this indicates that in approximately two-thirds of patients, the difference between the methods is expected to be ≤0.07 FFR unit, and roughly 20% of cases have a difference of ≥0.09 FFR unit. The tool's performance was consistent across levels of post-PCI FFR, with slightly higher mean differences in post-PCI FFR_{CT} Planner results of <0.80 (Supplemental Table 7). Post-PCI FFR should be interpreted as a continuous metric, with lower values associated with higher risk for adverse events.[6] Furthermore, the high accuracy of the FFR_{CT} Planner in patients with diffuse disease, a disease phenotype that represents a challenge for a percutaneous revascularization approach, is reassuring given the potential clinical usefulness of the FFR_{CT} Planner in these patients.

There is increasing awareness of the potential for coronary CTA to help plan and guide coronary interventions. Coronary CTA allows optimization of visualization angles in the catheterization laboratory, provides information on plaque morphology, and, through FFR_{CT}, provides lesion-specific functional evaluation of CAD.[24] This information allows for preprocedural, tailored planning of PCI in a fashion not previously possible. The FFR_{CT} Planner expands the use of coronary CTA from a diagnostic method to a planning tool for revascularization. Hence, the FFR_{CT} Planner may help clinicians better select patients to be referred to an invasive procedure, avoiding futile PCI and anticipating the benefit of an intervention. Another niche for this technology is inside the catheterization laboratory. The FFR_{CT} Planner may be beneficial in tandem stenosis cases to quantify the added value of stenting each of the lesions, and in cases of diffuse disease to maximize the benefit of the intervention while minimizing procedural risks and total stent length.[25] The present study validated the accuracy of the FFR_{CT} Planner in terms of post-PCI FFR. The impact of a PCI strategy guided by the FFR_{CT} Planner on clinical outcomes requires further investigation.

STUDY LIMITATIONS. First, this study was not powered to assess the impact of the FFR_{CT} Planner on clinical outcomes nor its clinical utility. The study validates the prediction of the planner in terms of post-PCI FFR, a recognized independent predictor of adverse events after PCI.[4-6] Second, PCIs were guided by OCT and FFR pullbacks to achieve the best result possible and to avoid the influence of suboptimal PCI results on the comparison with the predicted FFR_{CT} Planner. However, this approach may limit the generalizability of these findings to procedures performed with intravascular imaging and physiological guidance. Third, this approach may not be applicable to all lesion and patient subsets. Bifurcations with planned 2-stent strategies and left main coronary lesions were excluded; therefore, we cannot extrapolate these results to subsets of these lesion. Moreover, the accuracy of the FFR_{CT} Planner in cases of acute coronary syndromes, severely calcified vessels, bifurcation planned for 2-stent techniques, or aorto-ostial lesions, severe vessel tortuosity, previous revascularization, and in patients with atrial fibrillation requires further investigation. In addition, we recognize that female patients were underrepresented in this analysis. In clinical practice, the application of the FFR_{CT} Planner is limited to patients with epicardial vessels >1.8 mm. Fourth, the sites included in this study used the latest generation of CT scanners. The extrapolation of the present results to previous generation CT scanners requires further investigation. Finally, the FFR_{CT} Planner is a single-vendor commercial product, potentially limiting its generalized use.

CONCLUSIONS

Predicting the result of PCI is feasible using a tool based on coronary CTA and blood flow simulations. The FFR_{CT} Planner was accurate and precise for predicting FFR after PCI. The accuracy of the FFR_{CT} Planner was independent of CAD complexity and image quality. A randomized clinical trial investigating the clinical benefit of a PCI strategy guided by the FFR_{CT} Planner is warranted.

FUNDING SUPPORT AND AUTHOR DISCLOSURES

The study was sponsored by the Cardiac Research Institute Aalst with unrestricted grants from HeartFlow and Cardiopath. Drs Sonck and Munhoz have received research grants provided by the Cardiopath PhD program. Dr De Bruyne has received consultancy fees from Boston Scientific and Abbott Vascular; research grants from Coroventis Research, Pie Medical Imaging, CathWorks, Boston Scientific, Siemens, HeartFlow, and Abbott Vascular; and owns equity in Siemens, GE, Philips, HeartFlow, Edwards LifeSciences, Bayer, Sanofi, and Celyad. Dr Collet has received research grants from Biosensor, Coroventis Research, Medis Medical Imaging, Pie Medical Imaging, CathWorks, Boston Scientific, Siemens, HeartFlow, and Abbott Vascular; and consultancy fees from HeartFlow, OpSens, Abbott Vascular, and Philips Volcano. Dr Ko has received consulting fees from Canon Medical, Abbott, and Medtronic. Dr Mizukami has received consulting fees from Zeon Medical and HeartFlow; and speaker fees from Abbott Vascular. Dr Heggermont reports that Cardiac Research Institute Aalst receives consultancy fees on his behalf from Boston Scientific, Abbott Vascular, MicroPort, Medtronic, Biotronik, and AstraZeneca. Dr Updegrove and Ms Collinsworth are employees of HeartFlow. Dr Leipsic is a consultant and reports holding

stock options in Circle CVI and HeartFlow; and has received a research grant from GE and modest speaker fees from GE and Philips. Drs Norgaard and Møller Jensen have received unrestricted institutional research grants from Siemens and HeartFlow. Dr Otake has received research grants from Abbott Vascular; and speaker fees from HeartFlow and Abbott Vascular. Dr Ihdayhid has received consulting fees from Canon, Artrya Medical, and Boston Scientific. Dr Koo has received institutional research grants from HeartFlow. Dr Andreini has received research grants from GE Healthcare and Bracco. Dr Barbato has received speaker fees from Boston Scientific, Abbott Vascular, and GE. Dr Maeng has received advisory board and lecture fees from AstraZeneca, Bayer, Boehringer Ingelheim, Bristol Myers Squibb, Boston Scientific, and Novo Nordics; and research grants from Bayer and Philips Healthcare. All other authors have reported that they have no relationships relevant to the contents of this paper to disclose.

ADDRESS FOR CORRESPONDENCE: Dr Carlos Collet, Cardiovascular Center Aalst, OLV Hospital, Moorselbaan 164, Aalst 9300, Belgium. E-mail: carloscollet@gmail.com. Twitter: @ColletCarlos.

PERSPECTIVES

COMPETENCY IN MEDICAL KNOWLEDGE: Coronary CTA has evolved to a gatekeeper role for the evaluation of CAD. The addition of CT imaging–derived FFR has improved patient referral for PCI. The FFR_{CT} Planner enhances pre-procedural PCI planning and optimizes patient selection for percutaneous revascularization. This novel technology has been tested in a multicenter study confirming an accurate and precise prediction of the expected degree of functional revascularization.

TRANSLATIONAL OUTLOOK: The FFR_{CT} Planner could enhance patient selection and PCI planning, avoiding futile interventions. The impact of a PCI strategy guided by the FFR_{CT} Planner on clinical outcomes requires further studies encompassing complex anatomical CAD.

REFERENCES

1. Choi KH, Lee JM, Koo BK, et al. Prognostic implication of functional incomplete revascularization and residual functional SYNTAX score in patients with coronary artery disease. *J Am Coll Cardiol Intv*. 2018;11:237–245.

2. Lee JM, Hwang D, Choi KH, et al. Prognostic impact of residual anatomic disease burden after functionally complete revascularization. *Circ Cardiovasc Interv*. 2020;13:e009232.

3. Kobayashi Y, Lonborg J, Jong A, et al. Prognostic value of the residual SYNTAX score after functionally complete revascularization in ACS. *J Am Coll Cardiol*. 2018;72:1321–1329.

4. Lee JM, Hwang D, Choi KH, et al. Prognostic implications of relative increase and final fractional flow reserve in patients with stent implantation. *J Am Coll Cardiol Intv*. 2018;11:2099–2109.

5. Li SJ, Ge Z, Kan J, et al. Cutoff value and long-term prediction of clinical events by FFR measured immediately after implantation of a drug-eluting stent in patients with coronary artery disease: 1- to 3-year results from the DKCRUSH VII Registry Study. *J Am Coll Cardiol Intv*. 2017;10:986–995.

6. Piroth Z, Toth GG, Tonino PAL, et al. Prognostic value of fractional flow reserve measured immediately after drug-eluting stent implantation. *Circ Cardiovasc Interv*. 2017;10.

7. Fournier S, Ciccarelli G, Toth GG, et al. Association of improvement in fractional flow reserve with outcomes, including symptomatic relief, after percutaneous coronary intervention. *JAMA Cardiol*. 2019;4:370–374.

8. Agarwal SK, Kasula S, Hacioglu Y, Ahmed Z, Uretsky BF, Hakeem A. Utilizing post-intervention fractional flow reserve to optimize acute results and the relationship to long-term outcomes. *J Am Coll Cardiol Intv*. 2016;9:1022–1031.

9. Taylor CA, Fonte TA, Min JK. Computational fluid dynamics applied to cardiac computed tomography for noninvasive quantification of fractional flow reserve: scientific basis. *J Am Coll Cardiol*. 2013;61:2233–2241.

10. Nagumo S, Collet C, Norgaard BL, et al. Rationale and design of the Precise Percutaneous Coronary Intervention Plan (P3) study: prospective evaluation of a virtual computed tomography-based percutaneous intervention planner. *Clin Cardiol*. 2021;44:446–454.

11. Monizzi G, Sonck J, Nagumo S, et al. Quantification of calcium burden by coronary CT angiography compared to optical coherence tomography. *Int J Cardiovasc Img*. 2020;36:2393–2402.

12. Collet C, Katagiri Y, Miyazaki Y, et al. Impact of coronary remodeling on fractional flow reserve. *Circulation*. 2018;137:747–749.

13. Toth GG, Johnson NP, Jeremias A, et al. Standardization of fractional flow reserve measurements. *J Am Coll Cardiol*. 2016;68:742–753.

14. Collet C, Sonck J, Vandeloo B, et al. Measurement of hyperemic pullback pressure gradients to characterize patterns of coronary atherosclerosis. *J Am Coll Cardiol*. 2019;74:1772–1784.

15. Jang IK, Tearney GJ, MacNeill B, et al. In vivo characterization of coronary atherosclerotic plaque by use of optical coherence tomography. *Circulation*. 2005;111:1551–1555.

16. Bland JM, Altman DG. Statistical methods for assessing agreement between two methods of clinical measurement. *Lancet (London, England)*. 1986;1:307–310.

17. Bom MJ, Schumacher SP, Driessen RS, et al. Non-invasive procedural planning using computed tomography-derived fractional flow reserve. *Catheter Cardiovasc Interv*. 2021;97:614–622.

18. De Bruyne B, Pijls NH, Heyndrickx GR, Hodeige D, Kirkeeide R, Gould KL. Pressure-derived fractional flow reserve to assess serial epicardial stenoses: theoretical basis and animal validation. *Circulation*. 2000;101:1840–1847.

19. Biscaglia S, Uretsky B, Barbato E, et al. Invasive coronary physiology after stent implantation: another step toward precision medicine. *J Am Coll Cardiol Intv*. 2021;14:237–246.

20. Wolfrum M, De Maria GL, Benenati S, et al. What are the causes of a suboptimal FFR after coronary stent deployment? Insights from a consecutive series using OCT imaging. *EuroIntervention*. 2018;14:e1324–e1331.

21. Meneveau N, Souteyrand G, Motreff P, et al. Optical coherence tomography to optimize results of percutaneous coronary intervention in patients with non-ST-elevation acute coronary syndrome: results of the multicenter, randomized DOCTORS Study (Does Optical Coherence Tomography Optimize Results of Stenting). *Circulation*. 2016;134:906–917.

22. Collet C, De Bruyne B. FFR or OCT or FFR and OCT. *J Am Coll Cardiol Intv*. 2020;13:59–61.

23. Kim KH, Doh JH, Koo BK, et al. A novel noninvasive technology for treatment planning using virtual coronary stenting and computed tomography-derived computed fractional flow reserve. *J Am Coll Cardiol Intv*. 2014;7:72–78.

24. Collet C, Sonck J, Leipsic J, et al. Implementing coronary computed tomography angiography in the catheterization laboratory. *J Am Coll Cardiol Img*. 2021;14:1846–1855.

25. Modi BN, Sankaran S, Kim HJ, et al. Predicting the physiological effect of revascularization in serially diseased coronary arteries. *Circ Cardiovasc Interv*. 2019;12:e007577.

KEY WORDS coronary computed tomography angiography, FFR_{CT} Planner, fractional flow reserve, invasive coronary angiography, optical coherence tomography, percutaneous coronary intervention

APPENDIX For supplemental tables, figures, and case examples, please see the online version of this paper.